Next Materials 11 (2026) 101926

Contents lists available at ScienceDirect

Next Materials

journal homepage: www.sciencedirect.com/journal/next-materials

Research article

Performance of refractoriness geopolymer with alumina additive for ceramic weld backing applications

Pakamon Kittisayarm [a], Chayanee Tippayasam [b], Attaphon Kaewvilai [b], Kannika Thongma [a], Cristina Leonelli [c], Chanchana Thanachayanont [d], Greg Heness [a], Duangrudee Chaysuwan [a,*]

[a] Department of Materials Engineering, Faculty of Engineering, Kasetsart University, Bangkok 10900, Thailand
[b] Department of Welding Engineering Technology, College of Industrial Technology, King Mongkut's University of Technology North Bangkok, Bangkok 10800, Thailand
[c] Department of Engineering "Enzo Ferrari", University of Modena and Reggio Emilia, Via Pietro Vivarelli 10, Modena 41125, Italy
[d] National Metal and Materials Technology Center (MTEC), National Science and Technology Development Agency (NSTDA), Pathum thani 12120, Thailand

ARTICLE INFO

Keywords:
Geopolymer
Refractoriness
Alumina Powder
Ceramic Weld Backing
Potassium Alkali Solution

ABSTRACT

Back shielding gases are important for weld root quality in oxidation-sensitive materials. Metallic backing with gas venting is effective but heavy, costly, and limited in geometry and length, whereas ceramic backing is more suitable for controlling root shape than oxidation protection. Geopolymers offer a promising ceramic substitute with high thermal resistance and room-temperature processability. However, conventional MK–FA geopolymers have limited resistance when directly exposed to the intense heat of molten metal, which can be improved by alumina addition. This research focused on develop a thermally resistant and reusable geopolymer-based weld backing by tailoring alkali/pozzolan ratios (0.6–1.0) and incorporating alumina powder (0–15 wt%). Geopolymer specimens were examined in terms of compressive strength, refractoriness, microstructural development, thermal conductivity, and their performance during welding. The 0.6FM80A10 formulation was the best formula, offering the most balanced combination of properties. Its microstructure showed clear signs of densification, maintained phase stability even when exposed to temperatures approaching 1200 °C and lowest thermal conductivity (0.2645 W/m·K). Because of optimum alumina percentage helped tighten the matrix and reduce pore development, thereby strengthening the material and improving its resistance to high temperatures. After using 0.6FM80A10 as backing with venting gases in welding, the results showed that it had adequate heat efficiency, and it remained structurally sound through more than ten welding cycles. This research presented that the geopolymer with alumina additive could serve as sustainable weld backing with gas venting holes as an alternative to commercial metallic backing.

1. Introduction

Geopolymers are aluminosilicate-based materials that have emerged as a promising alternative to Portland cement due to their lower carbon footprint and the utilization of industrial byproducts such as fly ash and metakaolin [1–3]. In addition to environmental benefits, geopolymers exhibit excellent mechanical properties, thermal stability, and chemical resistance, making them suitable for structural and high-temperature applications [4–6].

One of the outstanding features of geopolymers is their ability to maintain structural integrity at elevated temperatures higher than 1000°C, outperforming many organic binders and several conventional ceramics [7–9]. This makes them potential candidates for components exposed to direct heat sources, including fireproof panels, thermal barriers and welding-related applications.

Back shielding gases are important in welding oxidation-sensitive materials such as stainless steel and aluminum. Normally, the backing gas is directly applied to the root side, while refractory aluminum foil is sometimes used in pipeline welding to control gas flow. For plate welding, metallic backings with gas venting achieve higher weld quality from more stable gas flow. However, it is short usable length, heavy weight, rigid geometry, and high cost limit their potential. Ceramic weld backings have been introduced as alternatives, but most designs remain solid and lack gas-venting features for controlled purge gas release. Therefore, the concept of developing a ceramic backing with gas-release holes is of particular interest. Geopolymers represent a promising

* Corresponding author.
E-mail address: fengddc@ku.ac.th (D. Chaysuwan).

https://doi.org/10.1016/j.nxmate.2026.101926
Received 24 October 2025; Received in revised form 8 March 2026; Accepted 14 March 2026
Available online 22 March 2026

Table 1
Chemical components of pozzolans.

Pozzolan	Chemical component (wt%)										
	SiO_2	Al_2O_3	Fe_2O_3	CaO	MgO	Na_2O	K_2O	SO_3	TiO_2	CO_2	LOI*
MK	53.81	39.97	1.35	0.02	0.06	0.05	2.25	0.02	0.06	2.24	0.17
FA	67.50	20.04	4.12	1.40	0.53	0.30	1.14	0.26	1.28	1.40	2.03

* Loss on ignition at 1050 °C

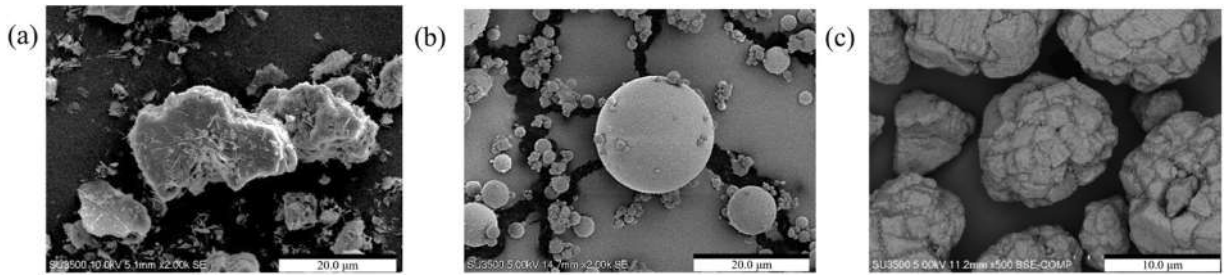

Fig. 1. Microstructure magnification of (a) kaolin (2000X), (b) fly ash (2000X) and (c) alumina powder (500X).

ceramic alternative due to their high thermal resistance and ease of fabrication at room temperature. However, typical metakaolin–fly ash (MK–FA) geopolymers exhibit poor direct contact with molten metal, which can be improved by alumina addition. Nevertheless, previous research on alumina-enhanced geopolymers has not fully addressed their applicability as weld backing nor optimized the combined effects of alkali-to-pozzolan ratio and alumina content on high-temperature performance [10–12]. In contrast, geopolymer-based weld backing offer significant advantages. Their excellent properties such as intrinsic thermal stability, refractory behavior, and ability to dissipate heat enable them to endure multiple welding cycles without damage [13–15].

Recent advances have demonstrated that reinforcing geopolymers with alumina (Al_2O_3) which is a refractory oxide with a melting point above 2000°C further enhances their heat resistance, microstructural densification, and thermal conductivity control [16–18]. Studies have shown that alumina-reinforced geopolymers are able to maintain compressive strength and dimensional stability even after repeated exposure to high temperatures [19–21]. However, most existing research has focused on general refractory applications, and little attention has been given to alumina-modified geopolymers as weld-backing materials that require both thermal insulation and structural stability across multiple welding cycles. The present research, therefore, aims to formulate an alumina-enhanced geopolymer suitable for weld-backing applications and to evaluate its high temperature performance and reusability potential for an aspect not addressed yet in previous research. Additionally, the integration of waste ceramics, nano-alumina, and fiber reinforcements further augments their mechanical integrity and eco-efficiency [22–25]. Moreover, geopolymers exhibit tailorable chemistry and phase morphology that can be optimized to meet the demands of specific applications, such as localized heating in welding operations. The ability to modify the SiO_2/ Al_2O_3 ratio, the choice of alkali activators, and incorporation of ceramic fillers like mullite or fine alumina aggregate allows precise control over thermal conductivity, shrinkage, and mechanical durability [26–28]. These tunable parameters provide a strategic pathway for designing heat resistant, cost-efficient, and reusable ceramic weld backing that meet the rigorous standards required in industrial welding environments [29, 30]. This research investigated the development of a reusable ceramic weld backing produced from alumina additive geopolymers by optimizing the alkali activator ratio and Al_2O_3 content. The main assumption of this research was that adding more alumina, together with selecting an alkali solution to pozzolans ratio that suited the system, would increase the high-temperature strength, limit firing shrinkage, and allow the material to withstand repeated welding. Accordingly, the primary research question focused on whether an alumina modified geopolymer could deliver sufficient thermal resistance, mechanical stability, and low thermal conductivity to function as a reusable weld backing material. To address this, we evaluated compressive strength at different temperatures, along with the material thermal conductivity, microstructural changes, and its reusability. The results showed that the optimized geopolymer offers better refractoriness and higher reusability than conventional ceramic weld backing.

2. Materials and methods

2.1. Aluminosilicate precursors and alkali activator

This research utilized metakaolin (MK) and fly ash (FA) as aluminosilicate precursors or pozzolans, selected for their high silica and alumina contents, as presented in Table 1. The kaolin used for metakaolin production was sourced from Mineral Resources Development Co., Ltd., in Ranong Province, Thailand. It was calcined at 650 °C for 2 h to transform to metakaolin, which was subsequently dried and ground. The resulting powder was then milled using a centrifugal ball mill to achieve a particle size smaller than 45 µm, corresponding to particles passing through a 325# sieve. Fly ash was provided by the Electricity Generating Authority of Thailand (EGAT), originating from the Mae Moh coal-fired power plant in Lampang. Additionally, high-purity alumina powder (99.40%, laboratory grade) was supplied by Colorobbia Holding S.p.A., Italy.

Scanning electron microscopy (SEM) (SU3500, Serial No: 351970–04, HITACHI, Japan) images (Fig. 1) revealed that kaolin exhibited irregular, angular particles with stacked platelet morphology. In contrast, fly ash particles were predominantly spherical and partly agglomerated due to combustion processes, while alumina powder showed rounded particles with rough surfaces forming aggregates. Furthermore, the chemical compositions of the pozzolanic materials (MK and FA) were determined by X-ray fluorescence (XRF) analysis using an XGT-5200 instrument (Horiba, Japan), as summarized in Table 3. The measured oxide contents were used to calculate the Si-to-Al and Na-to-Al molar ratios as critical indicators of the pozzolans reactivity.

The alkali activator comprised a 10 M potassium hydroxide (KOH) solution obtained from Daejung Chemicals & Metals Co., Ltd., and a commercial potassium silicate solution provided by C. Thai Chemicals

Table 2
Geopolymer mixtures for heat resistance.

Formulae	Alkali: Pozzolan	Pozzolan (g)		Alkali solution (g)		Additive (g)
		MK (g)	FA (g)	KOH (g)	K_2SiO_3 (g)	Al_2O_3 powder (g)
0.6FM60	0.6:1	60	40	30	30	0
0.6FM80		80	20	30	30	0
0.6FM100		100	0	30	30	0
0.8FM60	0.8:1	60	40	40	40	0
0.8 FM80		80	20	40	40	0
0.8 FM100		100	0	40	40	0
1FM60	1:1	60	40	50	50	0
1FM80		80	20	50	50	0
1FM100		100	0	50	50	0
0.6FM80A5	0.6:1	80	20	30	30	5
0.6FM80A10		80	20	30	30	10
0.6FM80A15		80	20	30	30	15

Co., Ltd., containing 10.83 wt% K_2O, 23.31 wt% SiO_2, and 65.86 wt% H_2O.

2.2. Geopolymer paste preparation

The alkali activator was prepared using a commercial potassium hydroxide solution and a 10 M potassium hydroxide solution, the latter produced by dissolving potassium hydroxide pellets in deionized water and allowing the solution to equilibrate for 24 h before use. Both solutions were mixed at 1:1 wt ratio. The alkali-to-solid ratios were varied at 0.6, 0.8, and 1.0 to determine the optimal mix. Once selected, alumina powder was added at 5, 10, and 15 wt% to enhance the refractoriness. Geopolymer pastes (Table 2) were formulated using different metakaolin-to-fly ash ratios (60:40, 80:20, and 100:0), with the Si: Al molar ratio maintained near 3 for the thermal performance. Each mixture was stirred to achieve homogeneity and cast into $25 \times 25 \times 25$ mm^3 acrylic molds (Fig. 2). Four replicate specimens were prepared for each formulation and each curing age in order to determine average values and standard deviations (mean ± SD). Specimens were covered with plastic film, cured at room temperature for 24 h. After demolding, the specimens were again wrapped with plastic film and subsequently stored in sealed containers until their designated testing ages.

2.2.1. Compressive strength

The compressive strength of each specimen stored was assessed at curing age durations of 7, and 28 days using a universal testing machine (UTM) (H50KS; Hounsfield; England). For each formulation, four replicate specimens were tested to obtain average values, and the test speed was controlled at 1 mm/min during compression. The compressive strength was calculated by dividing the maximum load by the cross-sectional area following ASTM C 109 [31].

2.2.2. Refractoriness

Geopolymer cubic specimens aged for 28 days were heated in the

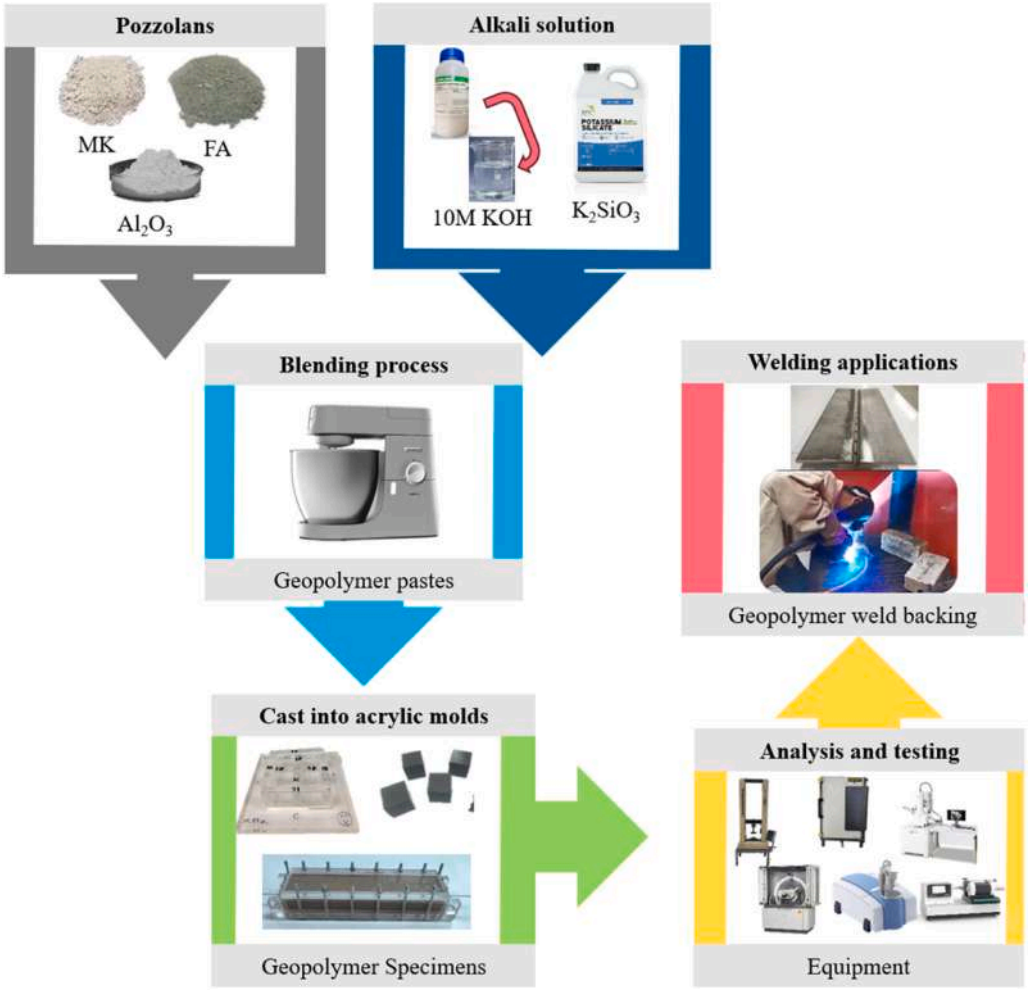

Fig. 2. Experimental procedure for geopolymer synthesis and weld backing application.

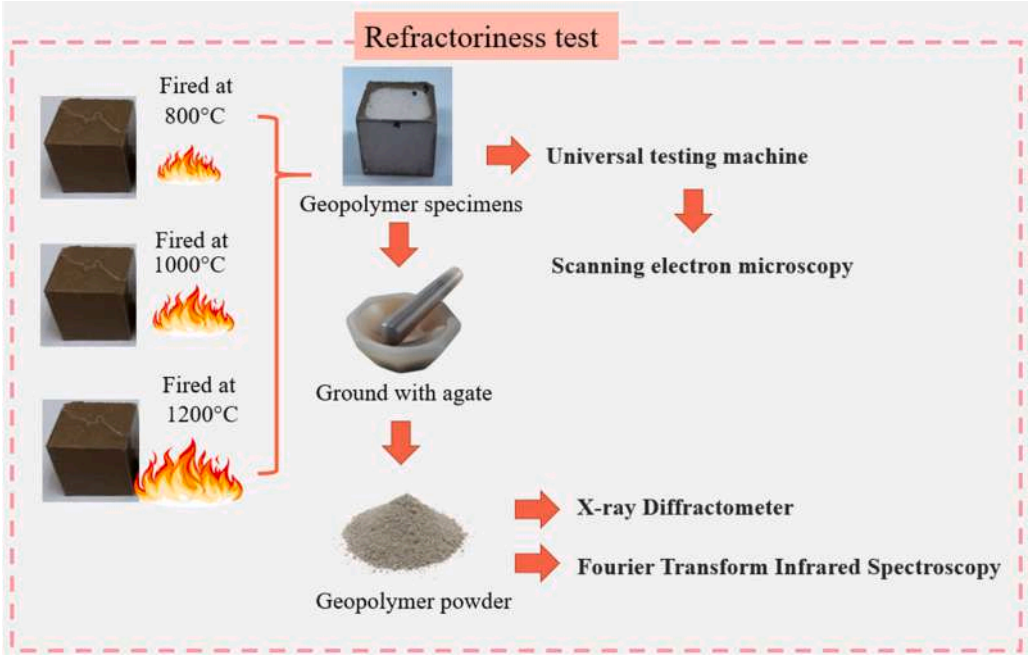

Fig. 3. Schematic illustration of the refractoriness and subsequent characterization of geopolymer specimens.

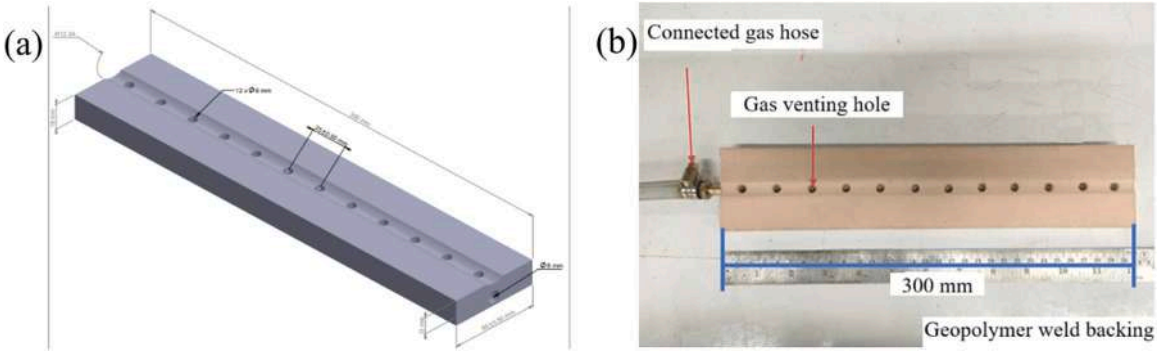

Fig. 4. (a) Dimensions and design of the 0.6FM80A10 rectangular geopolymer weld backing (b) Geopolymer weld backing with 12 gas venting holes and a connected gas hose.

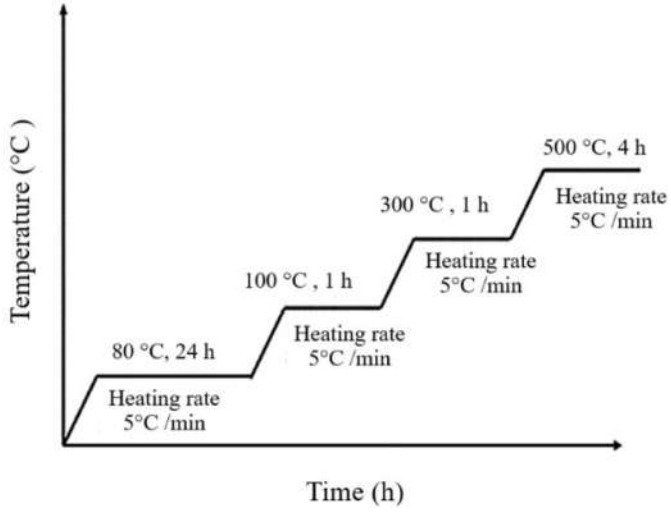

Fig. 5. Firing profile for organic removal from geopolymer weld backing [11].

Table 3
Welding parameters.

Parameters	Values
Distance between steel (root opening) (mm)	2.6
Travel speed (cm/min)	35–40
Current (A)	80–140
Voltage (V)	16.5–22
Ar gas flow rate (l/min)	10–15

furnace for 1 h at 800°C, 900°C, and 1200°C, with four replicate specimens tested per formulation at each temperature, using a controlled heating rate of 10 °C/min. After heating, the specimens were cooled to room temperature before high-temperature characterization. By comparing the size of the specimens before and after firing, the characteristics of the fired samples were examined, including compressive strength, XRD, FTIR, microstructure, and shrinkage (Fig. 3).

2.2.3. *Morphological analysis*

Scanning electron microscopy (SEM) was used to characterize the microstructures of raw materials, geopolymers, and other components in order to observe the morphology of the geopolymer matrix and the other

Fig. 6. Geopolymer weld backing in use, positioned beneath two stainless steel plates prepared for welding.

components of the structure developed. The SEM analysis was employed under 10–15.0 kV of accelerating voltage and 2000X magnification.

2.2.4. Identification of crystalline phases and IR spectrum

The crystalline phases of the geopolymer specimens were identified using X-ray diffraction (XRD) with a CuKα radiation source operated at 40 kV and 35 mA. The analysis was conducted with a step size of 0.02°, a counting time of 0.4 s per step, and a scan range of 5°–80° 2θ, resulting in a total scan duration of 45 min. The measurements were performed using an X′pert diffractometer (Philips, the Netherlands). In addition, fourier-transform infrared spectroscopy (FTIR) was carried out to investigate the functional groups present in the geopolymer matrix, using an Alpha-E instrument (Bruker, USA). The analysis was conducted in attenuated total reflection (ATR) mode with a wavenumber range of 500–4000 cm^{-1}, a spectral resolution of 4 cm^{-1}, and 64 scans collected for both the sample and the background. The resulting spectra were recorded in transmittance mode.

2.2.5. Coefficient of thermal expansion

A dilatometer was used to test the thermal expansion of geopolymer by heating the material through the volume and calculating the change in length as the temperature increased. The specimens were prepared into 0.5 × 0.5 × 2.5 mm^3 bar with a smooth tip. Each specimen was positioned horizontally and aligned parallel to the axis of length. The specimen was heated between 25 and 800 °C at a rate of 5 °C per minute in order to clarify the coefficient of thermal expansion (CTE). It was also possible to determine the transition temperature (Tg) and the softening temperature (Ts). Equation was used to determine the CTE of each specimen, as defined in Eq. (1) [32].

$$\Delta L = \alpha L_0 \Delta T \quad (1)$$

where L_0 is the original length
ΔL is the change in length
ΔT is the change in temperature
α is the coefficient of linear expansion

2.2.6. Thermal conductivity

Thermal conductivity (K), expressed in W/(m·K), indicates the rate at which heat transfers through a material, as defined in Eq. (2). A lower K value is desirable for ceramic-based materials such as geopolymers, especially for thermal insulation applications. In this research, the thermal conductivity of geopolymer specimens was measured using a thermal conductivity tester consisting of two plates at different temperatures. The specimen, with dimensions of 160 × 160 × 25 mm^3 at age of 7 days, were evaluated using three replicates per formulation to obtain average thermal conductivity values. Each specimen was positioned between the plates, and measurements were carried out at room temperature.

$$q = -K\frac{dT}{dx} \quad (2)$$

whereq is the heat flux (W/m^2)
K is the thermal conductivity (W/m·K)
$\frac{dT}{dx}$ is the temperature gradient (K/m)

2.2.7. Welding applications

The 0.6FM80A10 geopolymer was fabricated into a rectangular ceramic weld backing designed for welding applications, with dimensions of 300 × 60 × 18 mm^3 . A central groove with a 12.34 mm radius and 2 ± 0.5 mm depth was machined along the length to facilitate gas flow. Twelve gas venting holes, each 6 mm in diameter and 25 ± 0.5 mm apart, were drilled along the groove to ensure uniform gas distribution. A 6 mm gas-inlet hole was positioned at one end of the plate. The design is shown in Figs. 4 and 5.

The specimens were incubated at room temperature for 24 h, then unwrapped and cured for 7 days. Then, thermal treatment was performed as followed: drying at 80 °C for 24 h, calcining at 100 °C for 1 h,

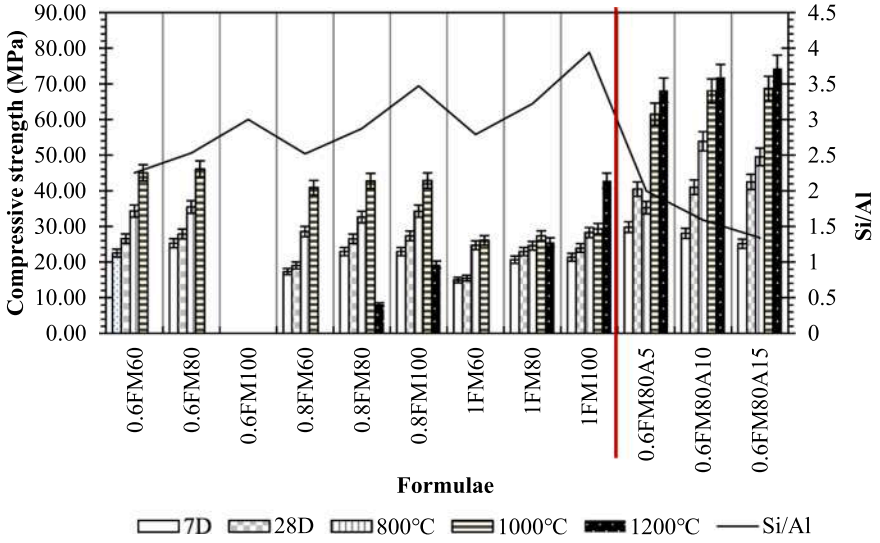

Fig. 7. Variation in compressive strength and Si/Al ratio of alumina additive geopolymers with different Fa/MK and alkali/pozzolan ratios at multiple firing temperatures.

Formulae	Before firing	After firing at 800°C	After firing at 1000°C	After firing at 1200°C
0.6FM80				
Note	Stable	Stable	Stable	Cracked
0.8FM80				
Note	Stable	Stable	Cracked	Broken
1FM80				
	Stable	Cracked	Cracked	Broken
Addition of aluminum powder				
0.6FM80 A5				
Note	Stable	Stable	Stable	Cracked
0.6FM80 A10				
Note	Stable	Stable	Stable	Stable
0.6FM80 A15				
Note	Stable	Stable	Stable	Stable

Fig. 8. Physical appearance of geopolymer specimens before and after refractoriness test at different temperatures with varying alumina contents Remarks: The evaluation was limited to macroscopic surface observation.

heating to 300 °C for 1 h, and firing at 500 °C for 4 h with a ramp rate of 5 °C/min to remove moisture and organic matters (Fig. 5).

Welding was performed using the parameters listed in Table 3, with travel speed of 35–40 cm/min and current between 80–140 A. The ceramic backings with gas-venting holes were used multiple times for different welded specimens on the same backing until either the ceramic fractured or oxidation appeared on the weld root. Three ceramic plates were tested in this study.

Before the welding test, the specimen was cured at 80 °C for 1 h, then aluminum tape was applied to the entire surface of the specimen to achieve good thermal conductivity and conduction of the specimen. The prepared specimen was positioned as a weld backing for tow stainless steel 304 plates used in the test. Steel specimens were prepared as butt joints with a single V-groove (75 × 300 × 6 mm). A root face of 3 mm and a root opening of 2 mm were maintained, with a groove angle of 60°. Filler metal AWS A5.9 ER308L (Ø 0.8 mm) was used, as shown in Fig. 6.

Table 4
ANOVA results and P-values for differences in compressive strength between geopolymer formulations.

Difference between ratio of	P values ($P_{x,y}$)	Level of significance	Summary of difference
		FA/MK	
0.6FM60 and 0.6FM80	$P_{(0.6FM60, 0.6FM80)} = 0.001843$	Significant ($P < 0.05$)	0.6FM80 exhibits noticeably higher compressive strength than 0.6FM60.
		Alkali /Pozzolan (FM80)	
0.6 and 0.8	$P_{(0.6,0.8)} = 0.001273$	Significant ($P < 0.05$)	The 0.6 ratio shows significantly higher compressive strength compared to 0.8.
0.8 and 1	$P_{(0.8,1.0)} = 0.000013$	Significant ($P < 0.05$)	Compressive strength decreases further when the ratio increases from 0.8 to 1.0.

Table 5
Comparative summary of precursor materials and mechanical performance in recent geopolymer refractory research.

Topic	Precursor	Mechanical performance
This research	Metakaolin and fly ash -based geopolymer with 5–15 wt% Al_2O_3 additive	Compressive strength up to 74 MPa after firing at 1200 °C
Comparative assessment of calcium aluminate cement and potassium metakaolin-based geopolymer as binders in high-alumina refractories [41]	Metakaolin -based geopolymer with tabular alumina and reactive alumina aggregates.	The geopolymer-bonded refractory (TA-4MK) reached its highest flexural strength of about 17 MPa after firing at 1250 °C.
Advanced solid geopolymer formulations for refractory applications [36]	Fly ash -based geopolymer with Al_2O_3 and mullite aggregates.	The geopolymer with mullite achieved a compressive strength of 84 MPa after firing at 1100 °C.
Geopolymers: a viable binder option for ultra-low-cement and cement-free refractory castables [37]?	Metakaolin-based geopolymer binder with tabular alumina, reactive alumina, and optional calcium aluminate cement (CAC).	The AT-3C-1G mix (2.7 wt% CAC + 1.3 wt% geopolymer) showed the best performance, with a flexural strength of 39.1 MPa at 1400 °C.
High-alumina refractory castables bonded with metakaolin-based geopolymers prepared with different alkaline liquid reagents [42]	Metakaolin-based geopolymer binder with tabular alumina, reactive alumina, and compare with NaOH- or KOH-based alkaline liquid.	The Na-based geopolymer 25.12 MPa and the K-based geopolymer 18.85 MPa at 1250 °C.
Effect of elevated temperatures on the performance of metakaolin geopolymer pastes incorporated by cement kiln dust [43]	Metakaolin-based geopolymer replaced with cement kiln dust (CKD)	MD20 (20% CKD replacement) reached about 35 MPa at ambient temperature and maintained 22.5 MPa after heating to 800 °C.
Controlling the thermal stability of kyanite-based refractory geopolymers [44]	Metakaolin-based geopolymer binder with calcined bauxite, calcined talc, and kyanite aggregates.	The highest flexural strength reached 45 MPa at 1200 °C using 80-μm kyanite aggregates.

3. Results

3.1. Compressive strength of geopolymer pastes with different ratio of alkali / pozzolan

The compressive strength results (Fig. 7) clearly showed that specimens exposed to elevated temperatures exhibited substantially higher strength than those tested at ambient conditions. This enhancement was strongly associated with the thermal property of aluminosilicate phases and the incorporation of Al_2O_3, both of which contributed to improve refractoriness and mechanical properties. The temperature increased from 800, 1000 and 1200 °C, the geopolymer matrix experienced progressive densification, characterized by the reduction of pore volume and the development of particle to particle bond strengthening through sintering. These microstructural transitions are consistent with previous research reporting that thermal exposure promotes structural rearrangement and the formation of thermally stable aluminosilicate networks in geopolymer refractories [33,34].

The 0.6FM80 increase in compressive strength at 800 and 1000°C, reflecting thermally induced densification and structural rearrangement. Although alkali activators were essential for precursor dissolution and geopolymerization or geopolymer gel formation, an excessive alkali to pozzolan ratio did not necessarily improve mechanical properties. In this research, the ratio of alkali to pozzolan of 0.6 provided sufficient dissolution to form a continuous aluminosilicate network while limiting the presence of excess free alkali. At higher activator ratios (0.8 and 1.0), the increased alkali content may have promoted the formation of alkali-rich amorphous phases and greater liquid phase generation during firing. At high temperatures, this excess alkali solution could volatilize, leading to differential shrinkage, microcracking and reduced structural stability [31]. This reason was consistent with the higher shrinkage and cracking observed during the refractoriness test (Fig. 8). Therefore, the superior strength of 0.6FM80 is attributed to an optimized balance between dissolution and thermal stability rather than simply reduced activator content [35]. The highest compressive strength observed in the 15 wt% Al_2O_3 was attributed to enhanced densification and increased Si-O-Al bonding, allowing greater porosity reduction and facilitating the formation of thermally stable phases, resulting in superior high temperature strength to those of 5 wt% and 10 wt% Al_2O_3 additions [36,37]. However, after the refractoriness test at 1200 °C, both 10 wt% (71 MPa) and 15 wt% (74 MPa) Al_2O_3 exhibited comparable compressive strength. It was found that the increasing alumina content by 5 wt% resulted in only an improvement of 3 MPa compressive strength, therefore, based on performance and structure efficiency, the 0.6FM80A10 (10 wt% Al_2O_3) formulation was selected for further investigation. It was also noted that 0.6FM100 formulation did not exhibit compressive strength results because its high viscosity prevented proper casting, and some mixes could not be sintered to 1200 °C due to thermal cracking during firing, making compressive strength testing infeasible.

3.1.1. Statistical validation of compressive strength using ANOVA

The compressive strength differences among the tested formulations were statistically verified through ANOVA (Table 4), with all compressive strength P-values below 0.05 [38–40]. The 0.6FM80 consistently outperformed 0.6FM60, while the 0.6 alkali/pozzolan ratio within the FM80 group presented significantly higher compressive strength than the 0.8 and 1.0 ratios. These results confirmed the reliability of the measured trends and supported the conclusions drawn from the mechanical tests.

3.1.2. Comparative overview of geopolymer refractory research

To provide a clearer context for this work's contribution, Table 5 outlines how the developed formulation compares to recent research on geopolymer-based refractories. The table summarizes the precursors and mechanical performance reported in related research, allowing the

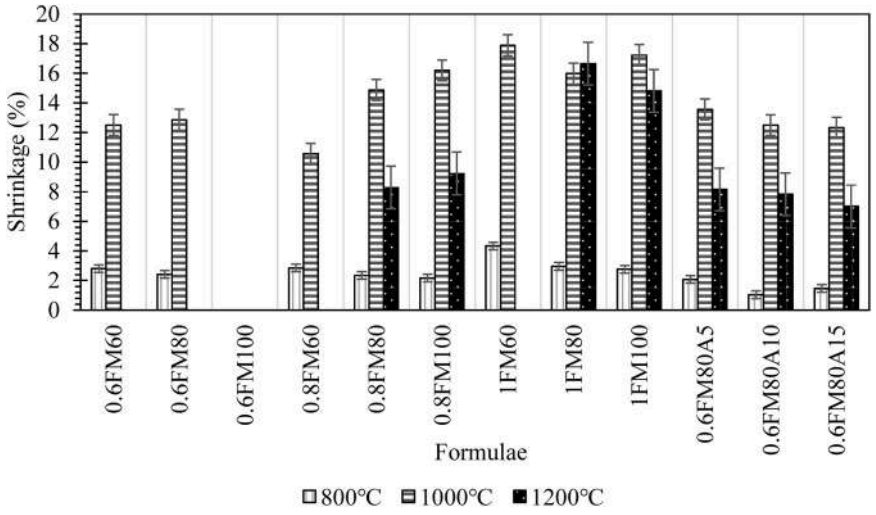

Fig. 9. Shrinkage behavior of alumina additive geopolymer pastes after firing at 800, 1000, and 1200°C.

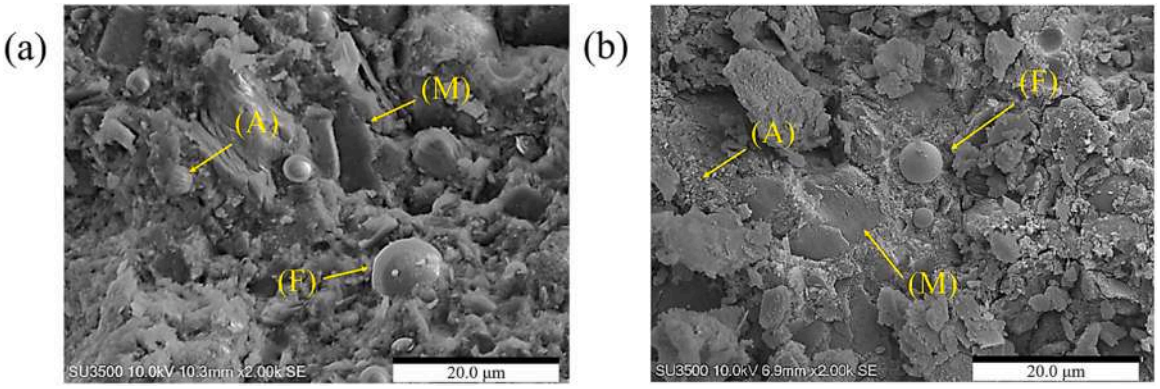

Fig. 10. SEM micrographs of geopolymer microstructure at 28 days for (a) 0.6FM80 and (b) 0.6FM80A10 formulations.

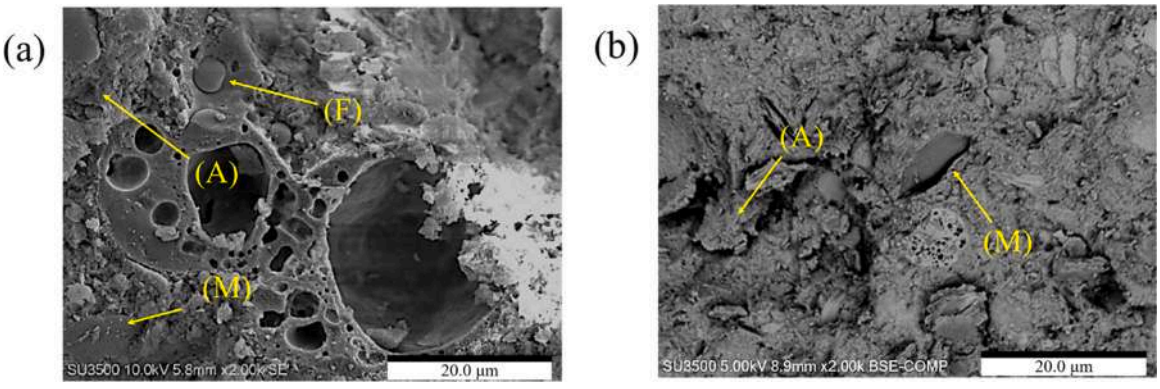

Fig. 11. SEM micrographs of geopolymer microstructure after firing at 800 °C (a) 0.6FM80 and (b) 0.6FM80A10.

results of this work to be placed in the context of current developments in geopolymer research.

3.2. Refractoriness of geopolymer pastes with different ratio of alkali/ pozzolan

Refractoriness, revealed that the ratio of alkali solution to pozzolanic material at ratios of 0.6:1 and 0.8:1 could withstand the heat unit 1000 ℃, because it was found that at 1200 ℃ specimens presented, cracking and fracturing occurred. The ratio of alkali solution to pozzolanic material at 1:1 was able to withstand the heat up to 800 ℃, as indicated in Fig. 8. Additionally, MK to FA ratios of 60:40 and 80:20 withstood temperatures up to 1000 ℃. When 5% aluminum powder was added to the mixture, minor cracking of specimens was observed. In formulations with 10% and 15% aluminum powder, the geopolymer specimens could withstand temperatures up to 1200 ℃ due to the high melting point of aluminum powder at 2054 ℃, thus the aluminum powder improved refractoriness.

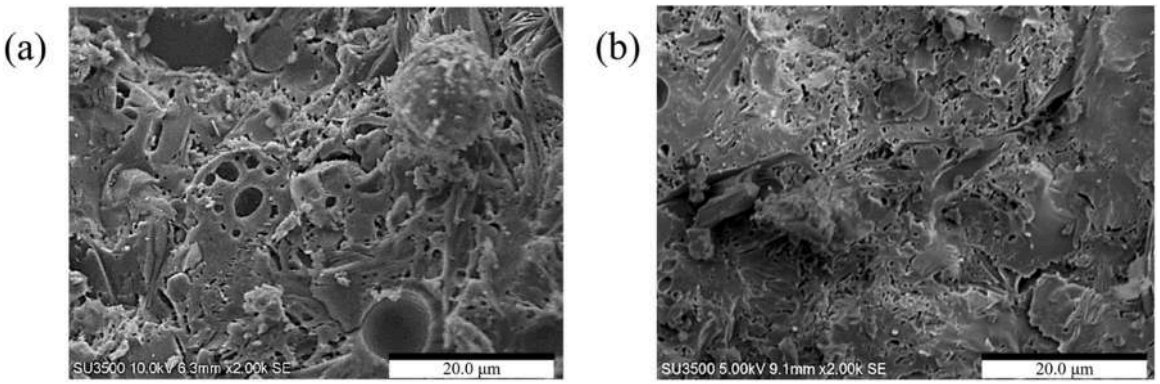

Fig. 12. SEM micrographs of geopolymer microstructure after firing at 1000 °C (a) 0.6FM80 and (b) 0.6FM80A10.

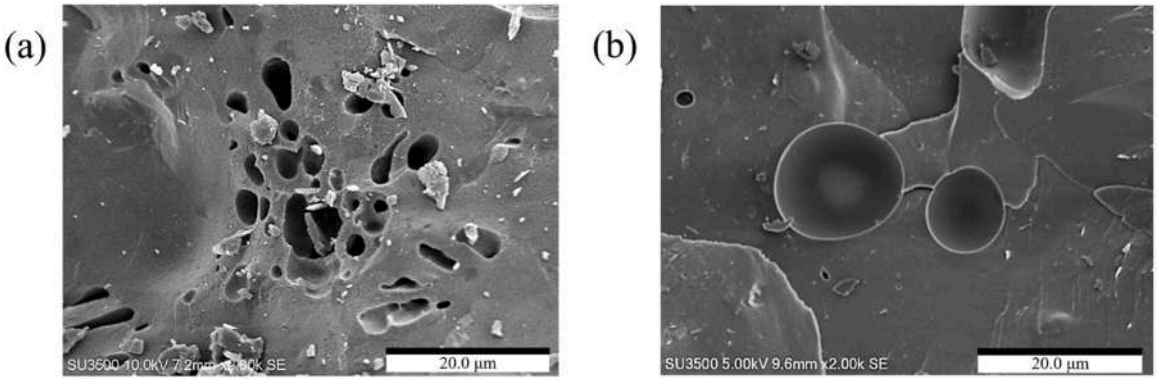

Fig. 13. SEM micrographs of geopolymer microstructure after firing at 1200 °C (a) 0.6FM80 and (b) 0.6FM80A10.

3.3. Firing shrinkage of geopolymer pastes

The shrinkage test after refractoriness, as shown in Fig. 9, indicated that the 0.8FM100 exhibited the lowest shrinkage, with a value of 2.17%, followed by the 0.6FM80, which had a shrinkage value of 2.43% when fired at 800°C. At this temperature, all formulations presented relatively low shrinkage, and the addition of Al_2O_3 powder further reduced shrinkage due to its high thermal resistance.

When refractoriness was reached at 1000 °C, the shrinkage values generally increased as a result of enhanced densification and further evaporation of bound water. However, the formulations containing Al_2O_3 still showed lower shrinkage compared to those without Al_2O_3, confirming the beneficial role of alumina in controlling dimensional changes.

At 1200 °C, only selected formulations remained intact, as some specimens failed to withstand this temperature and fractured during the firing process. For the surviving formulations, shrinkage values were higher than those observed at 800 and 1000 °C; however, the presence of Al_2O_3 effectively minimized the extent of shrinkage compared to the mixes without alumina.

3.4. Microstructure analysis

The microstructure of geopolymer paste at 28 days age, as shown in Fig. 10, was observed by SEM for the 0.6 FM 80 and 0.6FM80A10 formulas. Spherical FA particles (F) and plate-like MK particles (M) remained unreacted and unreacted particles were still visible alongside the formation of aluminosilicate gel (A). After firing at 800 and 1000 °C, as shown in Figs. 11 and 12, the microstructure revealed unreacted particles, aluminosilicate gel, and the development of pores due to partial decomposition of FA. At both temperatures, the formulation containing Al_2O_3 (0.6FM80A10) presented a denser and more consolidated matrix compared to the formulation without alumina (0.6FM80), confirming that the addition of Al_2O_3 promoted microstructural densification and mitigated pore formation under elevated temperatures. At 1200 °C (Fig. 13), the fly ash particles had completely decomposed, leading to the formation of a more homogeneous and compact microstructure. This densification, simultaneously occurred with the phase transformation of amorphous aluminosilicate into thermally stable crystalline phases, contributed directly to the increase in compressive strength observed at high temperature.

3.5. Chemical composition analysis

X-ray diffraction analysis, shown in Fig. 14 (a), was conducted on the 0.6MK80 geopolymer paste formula at 7 days of curing. Chemical components such as muscovite were identified, derived from MK [45], mullite, quartz from FA, and the alunite phase. After 28 days, similar components were observed, with an added potassium aluminum silicate phase formed through geopolymerization [46], confirming its classification as an aluminosilicate geopolymer material. A calcium silicate hydrate phase, a by-product of the geopolymerization, was also detected. X-ray diffraction of the 0.6MK80Al10 formula, as shown in Fig. 14 (b), revealed similar components, with an additional alpha-alumina phase enhanced heat resistance, given its high melting point of 2054°C.

Specimens fired at 800, 1000, and 1200°C retained phases present before firing, including quartz, and mullite, but lacked the potassium aluminum silicate phase, as alkali ions were released at elevated temperatures [47]. The alunite, kalsilite, and leucite phases emerged, indicating high heat resistance of the geopolymer paste [48], with melting points of 1750 and 1686°C, respectively.

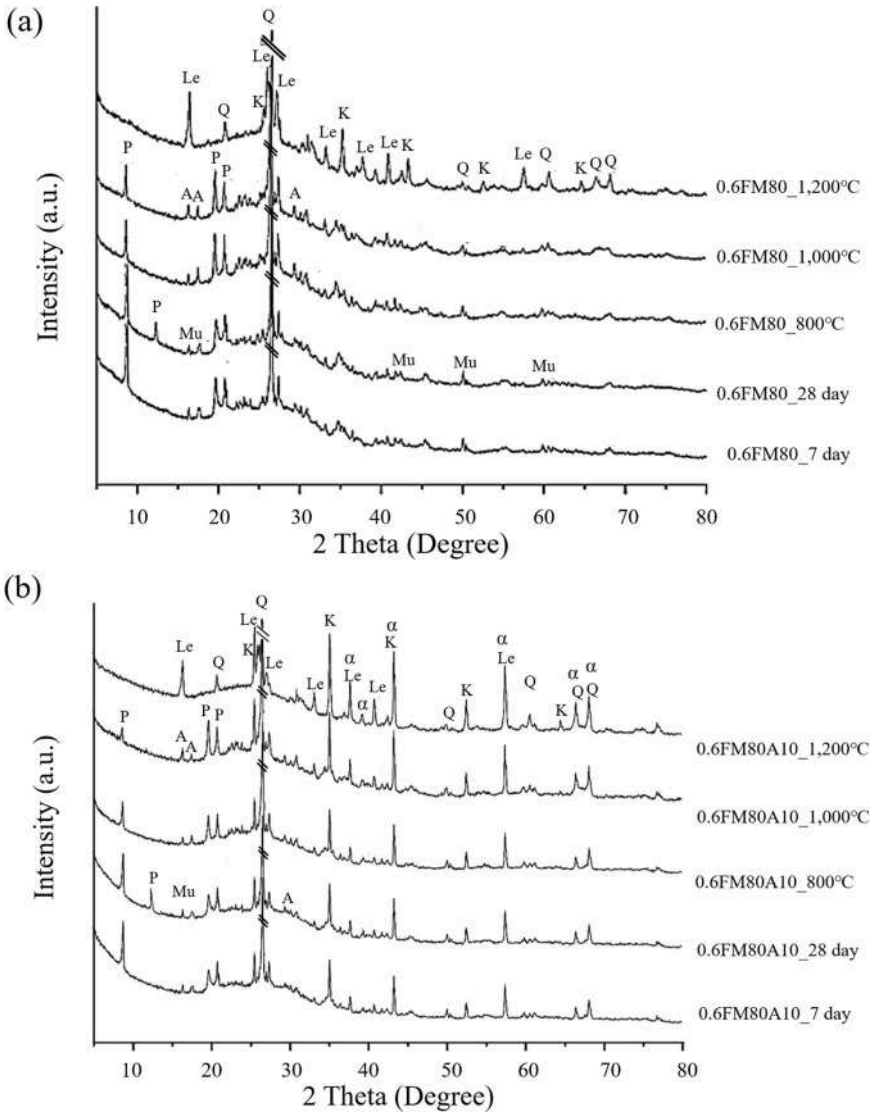

Fig. 14. XRD patterns of geopolymer specimens (a) 0.6FM80 and (b) 0.6FM80A10 at different curing ages and firing temperatures Q = Quartz (SiO_2, JCPDS 01–089–8934), Mu = Mullite ($3Al_2O_32Si_2$, JCPDS 00–001–1059), A = Alunite ($KAl_3(SO_4)_2(OH)_6$, JCPDS 00–003–0616), P = Potassium Aluminum Silicate ($AlKO_6Si_2$, JCPDS 00–051–1596), K = Kalsilite ($AlK(SiO_4)$, JCPDS 00–002–0297),Le = Leucite ($KAlSi_2O_6$, JCPDS 01–071–1147),α = Alpha-Alumina (Al_2O_3, JCPDS 01–088–0826).

3.6. Functional group analysis

The functional group analysis of geopolymer cured for 7 and 28 days, as shown in Fig. 15 (a) and (b), identified the functional groups of O-H, C-O, Si-O-(Si/Al), Si-O and Al-O. After firing at 800 and 1000 ℃, the functional groups C-O, Si-O-(Si/Al), and Si-O were still observed, while the O-H functional group was no longer present due to the heat causing the decomposition of water. Additionally, the height of the Si-O-(Si/Al) peak suggested that the geopolymerization reaction at 28 days was more complete than that at 7 days. This observation was consistent with the XRD results, where the formation of potassium aluminum silicate phases confirmed the geopolymerization process.

3.7. Coefficient of thermal expansion

The geopolymer paste specimens of 0.6FM80 and 0.6FM80A10, when subjected to a temperature of 900 ℃ with a heating rate of 10 ℃ per minute, exhibited thermal expansion coefficients (CTE) between 300 and 500 ℃ of 18.26×10^{-6} and 15.53×10^{-6} $℃^{-1}$, respectively. This demonstrated the effect of Al_2O_3 in reducing CTE due to its low thermal expansion characteristics. As shown in Fig. 16, within the temperature range of 0–130 ℃, there was dehydration in the structure without any shrinkage. The evaporation of water led to the initial shrinkage in the range of 130–450 ℃, where shrinkage occurred throughout the heating process until all water was evaporated. In the 450–700 ℃ range [49], the shrinkage was minimal because of the slow dehydroxylation of hydroxyl groups [50]. In the range of 700–800 ℃, slight expansion began [49].

3.8. Thermal conductivity

Geopolymer paste should had low thermal conductivity when used as a high-temperature-resistant material. Analysis of the thermal conductivity of the 28 days paste samples (in Table 6) revealed that the formula with Al_2O_3 (0.6FM80A10) gave the lowest thermal conductivity 0.2645 W/m·K, whereas, the one without Al_2O_3 had 0.3070 W/m·K. In comparison, Portland cement and firebrick refractory had thermal conductivity 1.019 [49] and 0.5000 W/m·K, respectively. The geopolymer pastes exhibited low thermal conductivity and met the standards of TIS 554. Therefore, the geopolymer paste 0.6FM80A10 was

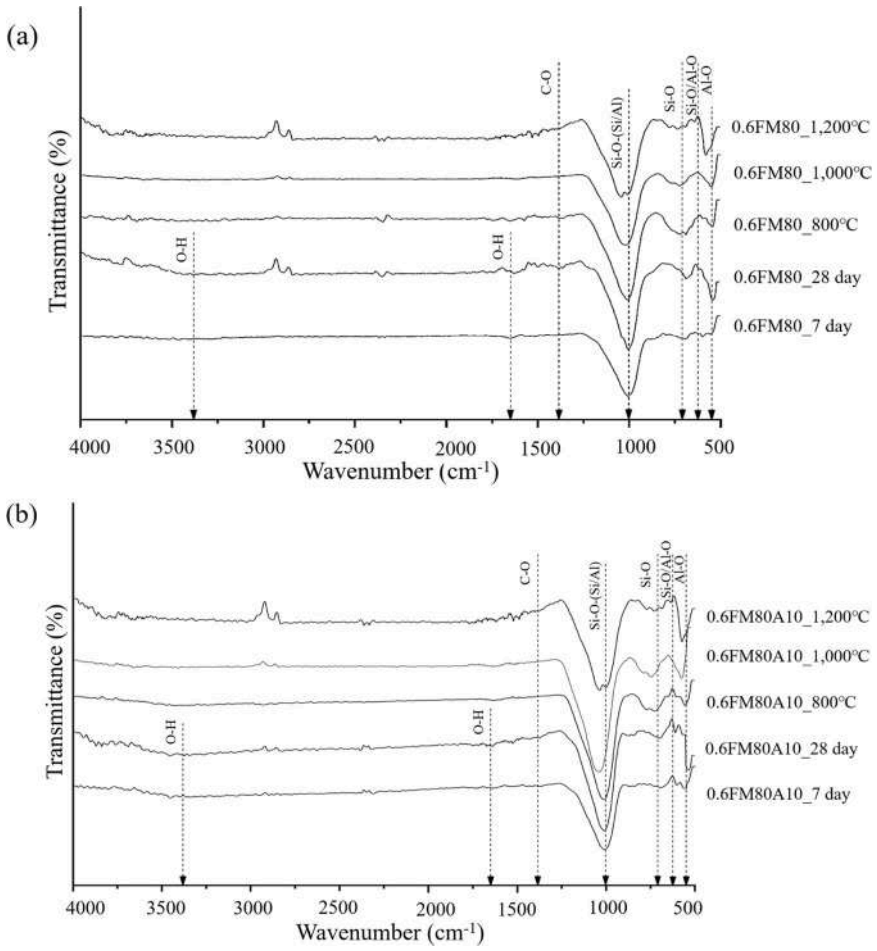

Fig. 15. FTIR spectra of geopolymer formulations (a) 0.6FM80 and (b) 0.6FM80A10 at different curing ages and firing temperatures.

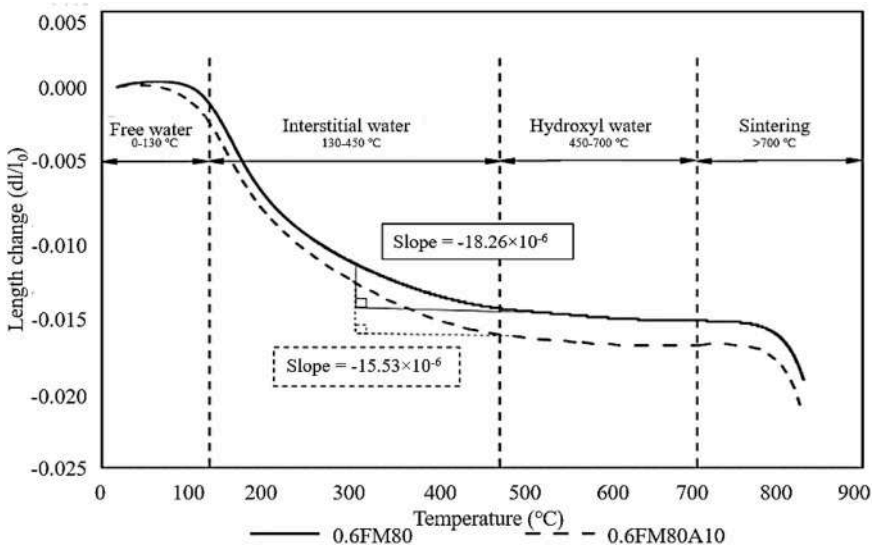

Fig. 16. Thermal expansion behavior of geopolymer formulations 0.6FM80 and 0.6FM80A10 during heating.

suitable for high thermal material applications, especially weld backing applications [51].

3.9. Welding test

After welding (Table 7), the inspection of ceramic weld backing call geopolymer weld backing (GWB) found that the wide curved backing from the geopolymer prototype demonstrated excellent heat absorption and dissipation. It was due to its ability to reduce heat accumulation from the covering gases released, resulting in minimal damage of the GWB. Consequently, it proved a cost-effective option because it could be reused more than 10 times.

Table 6
Thermal conductivity of geopolymer 0.6FM80 and 0.6FM80A10.

Formulae	Thermal conductivity (W/m·K)
0.6FM80	0.3070 ± 0.0021
0.6FM80A10	0.2645 ± 0.0331
Portland cement	1.019
Firebrick	0.5

4. Conclusions

This research offered high thermal resistance geopolymer formulated from MK-FA blended with an alkali-to-pozzolan ratio of 0.6 and Al_2O_3 addition with 10 wt% as novel backing with gas venting holes for oxidation-sensitive material welding. After firing at 1200 °C, the selected formulation remained stable and achieved compressive strengths above 70 MPa. This behavior reflected the role of alumina in densification, microstructure, and in improving its resistance to thermal

Table 7
Results of testing geopolymer weld backing.

Time	Geopolymer weld backing	Results of the inspection
1		Burn marks initiated
2		Slight burn increase, edge marks
3	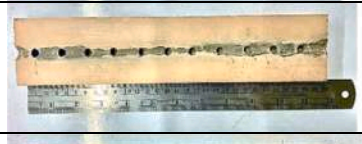	Splash at groove base, more burns
4	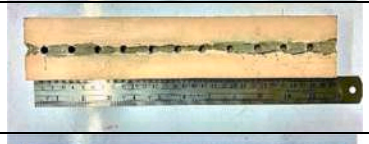	Increased splash and burn marks
5		More burns, minor edge cracks
6		Burns expanded, with edge cracks on both sides
7		Burn marks intensified
8		Severe burns, cracks at the support strip
9		Groove erosion deepens, cracks spread
10		Groove erosion, heavy burns, and more cracks

exposure. Its thermal conductivity of 0.2645 W/m·K also met the insulation threshold required by TIS 554, indicating suitability for high-temperature applications that require both strength and refractoriness. In practical use, the material performed effectively as a weld backing and endured more than ten welding cycles without cracking or loss of dimensional stability. Thus, alumina-addition geopolymers showed promise as durable, sustainable refractory materials and offer properties suitable for welding applications.

CRediT authorship contribution statement

Chayanee Tippayasam: Writing – review & editing, Methodology, Data curation, Conceptualization. **Kannika Thongma:** Methodology, Data curation. **Attaphon Kaewvilai:** Methodology, Conceptualization. **Pakamon Kittisayarm:** Writing – original draft, Methodology, Formal analysis, Data curation. **Chanchana Thanachayanont:** Investigation, Formal analysis. **Cristina Leonelli:** Validation, Conceptualization. **chaysuwan Duangrudee:** Writing – review & editing, Validation, Supervision, Resources, Project administration, Investigation, Funding acquisition, Conceptualization. **Greg Heness:** Investigation, Formal analysis.

Declaration of Competing Interest

The authors declare that they have no known competing financial interests or personal relationships that could have appeared to influence the work reported in this paper.

Acknowledgement

The authors are grateful to the Research and Innovation Fund, Faculty of Engineering, Kasetsart University, for research funds (Post Doc.68/10/MATE) and scholarship assistance and to Kasetsart University Research and Development Institute (KURDI), Bangkok, Thailand, for the revision of the English language by a native speaker. This work was financially supported by the Office of the Ministry of Higher Education, Science, Research and Innovation; and the Thailand Science Research and Innovation through the Kasetsart University Reinventing University Program 2021.

References

[1] M.A. Khasawneh, Geopolymer concrete in construction projects: a review, Discov. Civ. Eng. 2 (1) (2025) 1–20, https://doi.org/10.1007/s44290-025-00281-1.
[2] M. Liu, W. Dai, W. Jin, M. Li, X. Yang, Y. Han, M. Huang, Mix proportion design and carbon emission assessment of high strength geopolymer concrete based on ternary solid waste, Sci. Rep. 14 (1) (2024) 24989, https://doi.org/10.1038/s41598-024-76774-3.
[3] P. Kittisayarm, C. Tippayasam, C. Leonelli, C. Thanachayanont, A. Wannagon, G. Heness, D. Chaysuwan, Effective function of activated bagasse ash for high early strength geopolymer, J. Aust. Ceram. Soc. 60 (4) (2024) 1071–1083, https://doi.org/10.1007/s41779-024-01008-8.
[4] B.P. Bezerra, A.P. Luz, Geopolymers: A viable binder option for ultra-low-cement and cement-free refractory castables, Eur. Ceram. Soc. 44 (8) (2024) 5241–5251, https://doi.org/10.1016/j.jeurceramsoc.2024.02.013.
[5] T. Pantongsuk, C. Tippayasam, P. Kittisayarm, S. Nilpairach, D. Chaysuwan, Geopolymer synthesis using metakaolin and high calcium fly ash as binary system geopolymer, MSF 1007 (2020) 65–70, https://doi.org/10.4028/www.scientific.net/MSF.1007.65.
[6] S.G.K.M. Kumar, J.M. Kinuthia, J. Oti, B.O. Adeleke, Geopolymer Chemistry and Composition: A Comprehensive Review of Synthesis, Reaction Mechanisms, and Material Properties—Oriented with Sustainable Construction, Materials 18 (16) (2025) 3823, https://doi.org/10.3390/ma18163823.
[7] Y. Liu, X. Hu, Y. Du, B. Nematollahi, C. Shi, A review on high-temperature resistance of geopolymer concrete, J. Build. Eng. 98 (2024) 111241, https://doi.org/10.1016/j.jobe.2024.111241.
[8] R. Castillo, M. Ortega, J. Pérez, Factors affecting the compressive strength of geopolymers: A review, Minerals 11 (12) (2021) 1317, https://doi.org/10.3390/min11121317.
[9] S. Parzych, M. Paszkowska, D. Stanisz, A. Bąk, M. Łach, Possibilities of using geopolymers in welding processes and protection against high temperatures, Materials 16 (21) (2023) 7035, https://doi.org/10.3390/ma16217035.
[10] J. Murta, A.P. da Silva, C.E. dos Santos, D. Macanjo, H. Gomes, The effect of adding alumina to diatomaceous earth-based geopolymers, Eng. Proc. 56 (1) (2023) 328, https://doi.org/10.3390/ASEC2023-15907.
[11] S. Plaichum, A. Kaewvilai, T. Pantongsuk, D. Chaysuwan, C. Tippayasam, A novel ceramic backing strip from metakaolin-based geopolymer with gas flow holes for welding application, Key Eng. Mater. 856 (2020) 309–316, https://doi.org/10.4028/www.scientific.net/KEM.856.309.
[12] T.F. Santos, E.A. Torres, T.F. Hermengildo, A.J. Ramirez, Development of ceramic backing for friction stir welding and processing, Weld. Int. 30 (5) (2016) 338–347, https://doi.org/10.1080/09507116.2015.1096498.
[13] G. Masi, W.D. Rickard, M.C. Bignozzi, A. Van Riessen, The effect of organic and inorganic fibres on the mechanical and thermal properties of aluminate activated geopolymers, Compos B Eng. 76 (2015) 218–228, https://doi.org/10.1016/j.compositesb.2015.02.023.
[14] Q. Wei, Y. Liu, H. Le, Mechanical and thermal properties of phosphoric acid activated geopolymer materials reinforced with mullite fibers, Materials 15 (12) (2022) 4185, https://doi.org/10.3390/ma15124185.
[15] J. Bell, M. Gordon, W. Kriven, Use of geopolymeric cements as a refractory adhesive for metal and ceramic joins, Adv. Ceram. Coat. Ceram. Met. Syst. Ceram. Eng. Sci. Proc. 26 (2005) 407–413, https://doi.org/10.1002/9780470291238.ch46.
[16] R. Mohamed, M.M.A.B. Abdullah, R.A. Razak, T.L. Lee, T. Imjai, M.A.O. Mydin, D. L.C. Hao, geopolymers for fire protection applications, J. Mater. Sci. (2025) 1–32, https://doi.org/10.1007/s10853-025-11496-z.
[17] A. Harmaji, A. Adhikaprasetyo, B. Sunendar, Characterization of MgO and Al2O3 based Refractory waste as partial replacement for Fly ash based Geopolymer, Phys. Chem. Solid State 25 (2) (2024) 289–296, https://doi.org/10.15330/pcss.25.2.289-296.
[18] H. Shaik, S. Amritphale, J. Matthews, N. Paul, E. Matthews, R. Edwards, Advanced solid geopolymer formulations for refractory applications, Materials 17 (6) (2024) 1386, https://doi.org/10.3390/ma17061386.
[19] R.B.E. Boum, C.R. Kaze, J.G.D. Nemaleu, V.B. Djaoyang, N.Y. Rachel, P.L. Ninla, E. Kamseu, Thermal behaviour of metakaolin–bauxite blends geopolymer: microstructure and mechanical properties, SN Appl. Sci. 2 (8) (2020) 1358, https://doi.org/10.1007/s42452-020-3138-9.
[20] M. Amran, S.S. Huang, S. Debbarma, R.S. Rashid, Fire resistance of geopolymer concrete: A critical review, Constr. Build. Mater. 324 (2022) 126722, https://doi.org/10.1016/j.conbuildmat.2022.126722.
[21] W.M. Kriven, C.A. Kelly, D.C. Comrie, Geopolymers for structural ceramic applications, FA9550-04-C-0063, Air Force Off. Sci. Res. Rep. (2006). FA9550-04-C-0063.
[22] L. Qin, J. Yan, M. Zhou, H. Liu, A. Wang, W. Zhang, Z. Zhang, Mechanical properties and durability of fiber reinforced geopolymer composites: A review on recent progress, Eng. Rep. 5 (12) (2023) 1–22, https://doi.org/e12708.10.22541/au.166322346.64973526/v1.
[23] I. Hager, M. Sitarz, K. Mróz, Fly-ash based geopolymer mortar for high-temperature application–Effect of slag addition, J. Clean. Prod. 316 (2021) 128168, https://doi.org/10.1016/j.jclepro.2021.128168.
[24] H.S. Assaedi, M. D. Olawale, Impact of nano-alumina on the mechanical characterization of PVA fibre-reinforced geopolymer composites, JTUSCI 16 (1) (2022) 828–835, https://doi.org/10.1080/16583655.2022.2119735.
[25] M.H. Dheyaaldin, M.A. Mosaberpanah, R. Alzeebaree, Performance of fiber-reinforced alkali-activated mortar with/without nano silica and nano alumina, Sustainability 14 (5) (2022) 2527, https://doi.org/10.3390/su14052527.
[26] W. Liu, S. Ju, Tunable thermal conductivity of sustainable geopolymers by the Si/Al ratio and moisture content: Insights from atomistic simulations, J. Phys. Chem. B. 128 (12) (2024) 2972–2984, https://doi.org/10.1021/acs.jpcb.3c07445.
[27] G. Furtos, D. Prodan, C. Sarosi, D. Popa, M. Moldovan, K. Korniejenko, The precursors used for developing geopolymer composites for circular economy—A review, Materials 17 (7) (2024) 1696, https://doi.org/10.3390/ma17071696.
[28] T. Mingmuang, S. Lee, C. Thinvongpituk, Mechanical properties of aluminium-alumina welding by friction welding, Adv. Mater. Res. 418 (2012) 1279–1287, https://doi.org/10.4028/www.scientific.net/AMR.418-420.1279.
[29] N.A. Jaya, M.M. Al Bakri Abdullah, R. Ahmad, Reviews on clay geopolymer ceramic using powder metallurgy method, MSF 803 (2015) 81–87, https://doi.org/10.4028/www.scientific.net/MSF.803.81.
[30] T. Kovářík, D. Rieger, J. Kadlec, T. Křenek, L. Kullová, M. Pola, J. Říha, Thermomechanical properties of particle-reinforced geopolymer composite with various aggregate gradation of fine ceramic filler, Constr. Build. Mater. 143 (2017) 599–606, https://doi.org/10.1016/j.conbuildmat.2017.03.134.
[31] T. Pantongsuk, P. Kittisayarm, N. Muenglue, S. Benjawan, P. Thavorniti, C. Tippayasam, S. Nilpairach, G. Heness, D. Chaysuwan, Effect of hydrogen peroxide and bagasse ash additions on thermal conductivity and thermal resistance of geopolymer foams, Mater. Today Commun. 26 (2021) 102–149, https://doi.org/10.1016/j.mtcomm.2021.102149.
[32] P.P. Urone, R. Hinrichs, Coll. Phys. (Open.) (2012).
[33] M. Lahoti, K.K. Wong, K.H. Tan, E.H. Yang, Effect of alkali cation type on strength endurance of fly ash geopolymers subject to high temperature exposure, Mater. Des. 154 (2018) 8–19, https://doi.org/10.1016/j.matdes.2018.05.023.
[34] J.T. Gourley, G.B. Johnson, Developments in geopolymer precast concrete. World congress, Geopolymer Institute, Saint-Quentin, France, 2005, pp. 139–143.
[35] A.S.S.K. Mohammed, R. Géber, Effect of liquid-solid ratio on metakaolin-based geopolymer binder properties, Pollack Period. 20 (1) (2025) 110–116, https://doi.org/10.1556/606.2024.01141.

[36] S. Hussain, S. Amritphale, J. Matthews, N. Paul, E. Matthews, R. Edwards, Advanced Solid Geopolymer Formulations for Refractory Applications, Materials 17 (6) (2024) 1386, https://doi.org/10.3390/ma17061386.
[37] B.P. Bezerra, A.P. Luz, Geopolymers: A viable binder option for ultra-low-cement and cement-free refractory castables? J. Eur. Ceram. Soc. 44 (8) (2024) 5241–5251, https://doi.org/10.1016/j.jeurceramsoc.2024.02.013.
[38] Y.C. Chen, W.H. Lee, T.W. Cheng, Y.F. Li, A study on the shrinkage and compressive strength of GGBFS and metakaolin based geopolymer under different NaOH concentrations, Materials 17 (5) (2024) 1181, https://doi.org/10.3390/ma17051181.
[39] L.M.W. IV, D.A.M. Balingit, M.J.B. Espiritu, E.S. Cruz, Assessment of Workability, Compressive Strength, and Tensile Strength of Fly Ash-Glass Waste Fiber-Reinforced Geopolymer Concrete with Recycled Steel Can Fibers, Proc. 10th Int. Conf. Civ. Struct. Transp. Eng. 281 (2025) 1–8, https://doi.org/10.11159/iccste25.281.
[40] M. Asava-arunotai, T.L. Htet, A. Bansiddhi, A. Lertworasirikul, K. Surawathanawises, T. Muangnapoh, O. Jongprateep, 3D-Printed Sr-doped TiO_2/biowaste/polymeric structures for mitigating dye contamination in water, Materialia 36 (2024) 102139, https://doi.org/10.1016/j.mtla.2024.102139.
[41] B.P. Bezerra, A.P. Luz, Comparative assessment of calcium aluminate cement and potassium-metakaolin-based geopolymer as binders in high-alumina refractories, Cerâmica 71 (2025) 1–10, https://doi.org/10.1590/MKWV7164.
[42] B.P. Bezerra, A.P. Luz, High-alumina refractory castables bonded with metakaolin-based geopolymers prepared with different alkaline liquid reagents, Ceram. Int. 50 (11) (2024) 18628–18637, https://doi.org/10.1016/j.ceramint.2024.02.351.
[43] D. Ahmed, E. Kishar, Effect of elevated temperatures on the performance of metakaolin geopolymer pastes incorporated by cement kiln dust, Egypt. J. Chem. 64 (4) (2021) 1911–1926, https://doi.org/10.21608/ejchem.2021.50848.3041.
[44] J.G.N. Deutou, R.C. Kaze, E. Kamseu, V.M. Sglavo, Controlling the thermal stability of kyanite-based refractory geopolymers, Materials 14 (11) (2021) 2903, https://doi.org/10.3390/ma14112903.
[45] C. Tippayasam, P. Balyore, P. Thavorniti, E. Kamseu, C. Leonelli, P. Chindaprasirt, D. Chaysuwan, Potassium alkali concentration and heat treatment affected metakaolin-based geopolymer, Constr. Build. Mater. 104 (2016) 293–297, https://doi.org/10.1016/j.conbuildmat.2015.11.027.
[46] W.D. Rickard, A.V. Riessen, P. Walls, Thermal character of geopolymers synthesized from class F fly ash containing high concentrations of iron and α-quartz, Int. J. Appl. Ceram. Technol. 7 (1) (2010) 81–88, https://doi.org/10.1111/j.1744-7402.2008.02328.x.
[47] P. Duxson, G.C. Lukey, J.S. van Deventer, The thermal evolution of metakaolin geopolymers: Part 2–Phase stability and structural development, J. NonCryst. Solids 353 (22-23) (2007) 2186–2200, https://doi.org/10.1016/j.jnoncrysol.2007.02.050.
[48] D.S. Perera, R.L. Trautman, Geopolymers with the potential for use as refractory castables, ATM 7 (2) (2005) 187–190, https://doi.org/10.2240/azojomo0173.
[49] P. Jittabut, P. Chindaprasirt, S. Pinitsoontorn, The study of physical and thermal conductivity properties of cement paste containing nanosilica, Key Eng. Mater. 659 (2015) 164–168.
[50] P. Duxson, G.C. Lukey, J.S. van Deventer, Thermal evolution of metakaolin geopolymers: Part 1–Physical evolution, J. NonCryst. Solids 352 (52-54) (2006) 5541–5555, https://doi.org/10.1016/j.jnoncrysol.2006.09.019.
[51] A. Kaewvilai, P. Kittisayarm, T. Thaweechai, G. Heness, C. Leonelli, D. Chaysuwan, C. Tippayasam, Heat-resistant geopolymer derived from metakaolin–fly ash blend with bagasse ash addition: an innovative curved backing for steel pipe welding, J. Aust. Ceram. Soc. (2025) 1–18.